

# Health Estimation of Magnetic Wheel Encoder

Jasmeet Singh Ladoiye<sup>1</sup>, Douglas Spry<sup>2</sup>, and Milad Jalali<sup>3</sup>

<sup>1,3</sup>*General Motors Company, Canadian Technical Center, Markham, Ontario, L3R 4H8, Canada*

*Jasmeets.ladoiye@gm.com  
Milad.jalali@gm.com*

<sup>2</sup>*General Motors Company: Milford Proving Grounds, Milford, Michigan, 48380, USA  
Douglas.spry@gm.com*

## ABSTRACT

Performance of several vehicle safety features, such as anti-lock brake system (ABS), traction control system (TCS) and electronic stability control (ESC) rely on the quality of the wheel speed signal. One potential failure mode for the wheel speed encoders is gradual deposition of foreign paramagnetic debris on the surface of the magnetic encoder. This results in reduced strength of the magnetic field and impacts the quality of the wheel speed signal. Noisy wheel speed signals may lead to false activations or poor performance of ABS, leading to poor drivability, longer brake distance, etc. Therefore, it can negatively impact several safety critical features and the customer's experience.

Data collected from several faulty encoders with various levels of faults were used to develop the prognostics methodology proposed here to evaluate a magnetic wheel encoder's health. This method leverages time domain and frequency domain-based health indicators to monitor the deterioration in wheel encoder. Time domain-based health indicators include VDA (Verband der Automobilindustrie) signals that are generated by advanced wheel speed sensors, and an enveloping filter of the wheel speed signal's noise. The frequency domain-based health indicator include root mean square amplitude of average order spectrum of wheel speed noise. The performance of individual health indicators as well as a combination of them are compared to assess the separation between healthy and degraded encoders. Results indicate that the degradation process due to magnetic debris accumulation can be monitored using the proposed method.

## 1. INTRODUCTION

In recent years, prognostics and health management systems gained importance in organizations throughout the world to

maximize performances and guarantee uptime of various systems/sub-systems. Prognosis involves health indicator (HI) generation by using data from the sensors of the monitored system. Further maintenance-based decisions can be taken by detecting anomalies in the performance of the HI.

Sensors play an important role in the generation of HI's of the modern systems. Any sensor related failures impact the quality of sensing data and can lead to unexpected results deviated from the normal conditions. A very healthy literature review of various fault detection and isolation applications (FDI) is available that focuses on the model-based detection approaches to identify the faults: Kim, Setiawan, and Pratama, 2014 and Clark, Frank, and Patton, 2000.

Antilock braking system (ABS) was introduced in the 1920s in the aviation industry and later was extended to the automotive industry. The performance of the ABS on conventional vehicles are of huge significance and has gone through various improvements in the last two decades (Chen, Liu, and Jing, 2011, Kaynak, Kayacan, and Oniz, 2009, Cantoni, Tanelli, and Savaresi, 2006). Features such as ABS, TCS and ESC ensure vehicle stability in challenging conditions such as cornering, braking with low surface friction capacity, etc. and the performance of these features is heavily reliant on wheel speed information. The industry standard for wheel speed sensing is comprised of a wheel speed sensor (WSS, also called sensing element) and rotating magnetic element (also called wheel encoder, magnetic encoder, and ABS tone ring) fitted on each wheel corner assembly as shown in Figure 1. The rotating magnetic encoder produce magnetic flux through the sensing element and indicates wheel motion which can be used to calculate a wheel's speed (Dadashnialehi, 2013). Hence, it is critical to provide an accurate measurement of wheel motion to provide a reliable wheel speed for use by safety critical features in order to avoid false activations, increased brake distance, etc.

Any deterioration in the health of the WSS, wheel encoder and/or the interface between the sensor and encoder impacts

Jasmeet Ladoiye et al. This is an open-access article distributed under the terms of the Creative Commons Attribution 3.0 United States License, which permits unrestricted use, distribution, and reproduction in any medium, provided the original author and source are credited.

the quality of the wheel speed signal. Several attempts have been made to improve the accuracy of WSSs using data-processing. Irregularities in the gap between WSS and wheel encoder also impacts the quality of the wheel speed signal (Isermann, Scheerer, Nelles, and Schwarz, 1997). An adaptive filter based on least squares method was also proposed to improve the performance of the WSS (Hernandez,2003). A noise mitigation strategy was proposed by the same author using an adaptive line enhancer algorithm to filter wheel speed information from noisy wheel speed signals (Hernandez,2003).

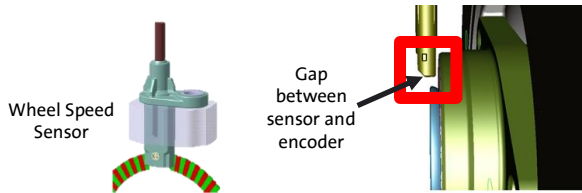


Figure 1. Description of WSS and encoder interface

The wheel encoder is also susceptible to environmental and operational factors such as during repairs or inspections (Dadashnialehi,2013). Common wheel encoder failures which impact the quality of the wheel speed signal include missing teeth, blended poles, and deposition of magnetic debris. A failure is categorized as missing teeth if a tooth or number of teeth gets eroded due to some impact on the encoder. A defect where one or more teeth of the encoder is demagnetized by meeting some permanent magnet such that poles becomes are not distinguishable is termed as blended poles. Deposition of paramagnetic debris on the surface of the wheel encoder also presents a potential failure mode. Causes of failure modes such as missing teeth and blended poles are instant in nature while the latter happens gradually and falls in scope of prognostics.

Hence, any potential failures related to the WSS/encoder interface poses threat to the functionality of the safety control features. The presence of the failures may deteriorate slip regulation and will result in inaccurate or insufficient control.

Most of the prior work around WSS focused on mitigation of the wheel noise through data-processing. The major contributions of this work are that, unlike the previous this work focuses on the following aspects: To ensure the proper functioning and maximizing the availability of the safety critical features, a fault detection approach is developed to prognose the faults related to wheel encoder. The details are as follows:

1. HIs based on VDA: AK protocol, wheel speed noise: Envelope filter and wheel speed noise: Order analysis are developed.

2. Explored the limitations of each of these HIs and developed a fused indicator by using all the above-mentioned indicators.
3. Results demonstrate the capability of each of HIs to detect contaminated encoders.

This paper is organized as follows: Section 2 focuses on the fault injection of the encoders along with the experimental setup for data collection, Section 3 describes the approach to determine the HI's and also discuss the ground truth generation of encoders, Section 4 discusses the experimental results and Section 5 outlines the conclusion.

## 2. DATA COLLECTION

This section details the fault injection procedure on the wheel encoder and data acquisition setup to collect the data from samples and predict the health of the wheel encoder.

### 2.1. Fault Injection

To create the faulty contaminated encoders, healthy encoders were injected with fine depositing of iron shavings on the surface of the wheel encoder as shown in Figure 2. It is important to glue paramagnetic material to the surface of encoder to evaluate the impact of deposition on the HI's, otherwise heavy particles or particles with low paramagnetic properties will flyoff.



Figure 2. Fault injection on healthy samples to produce contaminated encoders.

Case ID	FaultMode
97	Healthy 2.5 mm
118	Healthy 1 mm
117	Healthy 1 mm
121	Healthy 2 mm
122	Healthy 2 mm
213	Magnetic Debris 1.0g
220	Magnetic Debris 0.6g
218	Magnetic Debris 1.8g
219	Magnetic Debris 0.6g
217	Magnetic Debris 1.8g
215	Magnetic Debris Teeth covered

Table 1. List of healthy and faulty encoders

The procedure of fault injection is repeated on healthy samples to produce faulty encoders of various amount of debris. Table 1 illustrates the list of healthy and faulty

encoders created to perform the study. Healthy samples were recorded at set gap of 1,2, and 2.5 mm whereas contaminated encoders were tested at set gap of 2.5 mm as shown in Table 1. The quantity of the magnetic debris does not impact the quality of wheel speed linearly but in fact it depends on the distribution of debris over the encoder.

It is important to collect data at various speeds and accelerations. Therefore, to avoid the debris falling off at high speeds, the debris is glued to the surface of the encoder as shown in Figure 2. Adhering the debris will also prevent flying debris contaminating the testing environment.

**2.2. Experimental Setup**

Various tests were conducted on a WSS bench to study the impact of debris on wheel encoders. The WSS bench has capability to change the gap between WSS and wheel encoder using a speed and gap simulator as shown in Figure 3. The bench is equipped with an active WSS with AK Protocol to do the data recording. Therefore, information about wheel position is encoded by three (7 mA, 14 mA and 28 mA) current levels. (Vachtsevanos, Lewis, Roemer, Hess, & Wu (2006)). The bench is connected further to the HIL (Hardware-in-loop) setup and the data is collected through an EBCM (Electronic Brake Control Module). A total of 38 tests were conducted out of which 22 tests were done with healthy samples at different gap settings (1,1.5,2 & 2.5 mm) and 13 tests using contaminated encoders at 1 mm of gap to collect approximately of 836 minutes of data.

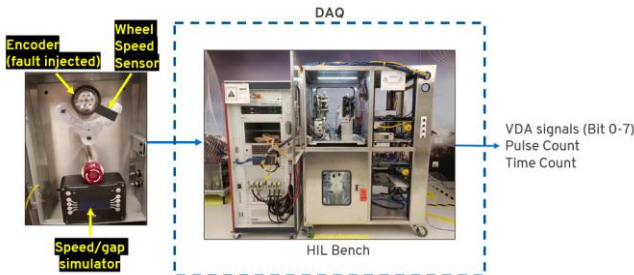


Figure 3. WSS bench setup

Data from the EBCM is acquired in .dat format with sampling frequency of 200 Hz using ETAS INCA tool and further exported to MATLAB 2020a for analysis. VDA signals, pulse count and time count are the main signals of interest necessary to develop the concepts further.

**3. ALGORITHM DEVELOPMENT**

Pulse count and time count are used to determine wheel speed of the corner by using Eq.1. Wheel speed is further processed in time and frequency domain along with VDA signal to produce signatures used to determine the degradation. These signatures are termed as Health Indicators and can be used to differentiate between healthy and degraded encoder.

$$\text{Wheel Speed} = \frac{\Delta \text{Pulse Count}}{\Delta \text{Time Count}} * \frac{\text{Effective Circumference}}{\text{Tooth Count}} \quad (1)$$

Where:

Wheel Speed = Speed of wheel in rps (revolutions per second)

Teeth Counts = Number of teeth of encoder ~ 96

Effective Circumference = Distance required to complete one rotation

**3.1. Health Indicators**

The conditioned data collected from the WSS is processed further to generate HIs. These individual indicators are further accessed to identify the health of the system. Figure 4 illustrates the summary of the HI's developed.

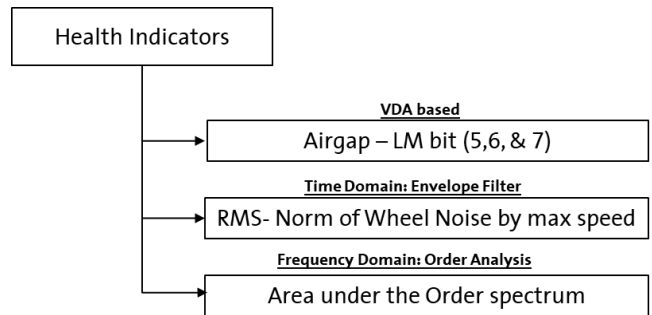


Figure 4. Health Indicators

**3.1.1. VDA**

Unlike traditional sensors, Active WSS produce a speed pulse along with nine data protocol bits whenever an edge teeth on wheel encoder is detected known as AK Protocol as shown in Figure 5 (Vachtsevanos, Lewis, Roemer, Hess, & Wu, 2006).

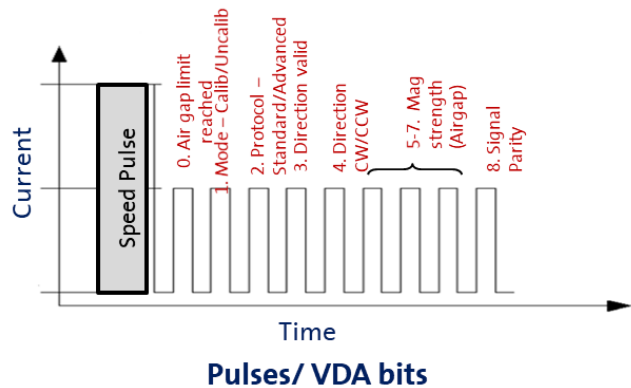


Figure 5. Description of VDA bits outputted from AK Protocol based WSS

AK protocol contains information related to magnetic strength of the signal, sensor calibration mode, encoder sense

of rotation and parity. These data protocol bits are binary in nature and are embedded with information that can be utilized further to develop diagnostics and prognostics around it. Additional information related to each bit is provided in the Table 2.

The quality of the wheel speed signal depends on the magnetic strength. Any deterioration in the health of the wheel encoder will also impact the magnetic strength of the signal. Therefore, presence of magnetic debris on the surface of the encoder will hamper the quality of wheel speed signal. VDA bits 5-7 which can be converted to a 3-bit integer (7-Maximum magnetic strength, 0-Minimum magnetic strength) which correlates to the magnetic strength at the interface and shows potential to determine faults at the interface.

Bit	Name	Description
0	Airgap Reserve	1 Magnetic strength too low to stay in normal mode
1	Status Mode	0 Calibrated Mode, 1 Uncalibrated Mode
2	Advanced Protocol	1 Transmission of advanced AK protocol is enabled
3	Validity of Direction of Rotation	1 if Direction is valid
4	Direction of Rotation	0 if clockwise, 1 if anticlockwise
5	LM0 (LSB)	Gap indication, lowest significant bit
6	LM1	Gap indication, medium significant bit
7	LM2(MSB)	Gap indication, most significant bit
8	Parity	1 for even parity, P = XOR (bit 0 to bit 7)

Table 2. Definition of VDA-AK protocol

### 3.1.2. Envelope of Wheel Speed

The envelope of a signal is a smooth trace outline the upper and lower bounds of the signal. The quality of the wheel speed signal is quantified in terms of wheel speed noise i.e. the difference between the upper envelope and lower envelope as given in Eq. 2.

$$\text{Wheel Speed Noise} = \text{Upper Envelope} - \text{Lower Envelope} \quad (2)$$

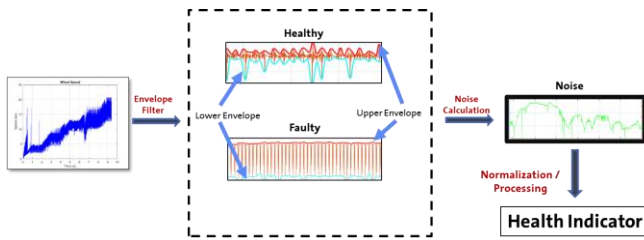


Figure 6. Wheel speed noise determination using envelope filter of the wheel speed signal.

Faults on the wheel encoder impacts the quality of the wheel speed signal. Therefore, a faulty encoder will produce a noisy wheel speed signal in comparison to a healthy encoder, with the magnitude of the noise depending upon the severity of the fault. Wheel speed noise is detrended further by normalizing with the median buffer speed and taking the root-mean-square (RMS) noise in the buffer length as show in in Figure 6. It is important to do processing of wheel noise to make it independent of the changes in wheel speed signal.

### 3.1.3. Average Order Spectrum (AOS) of wheel noise

The noise in the wheel speed is further analyzed in frequency domain using order analysis. Each order refers to a frequency that is a fixed multiple of rotational speed. In this case, first order refers to the number of events per each revolution of the wheel.

A short-time Fourier transform of the wheel noise is done to get a spectral map of order as a function of RPM averaged over time. Average order spectrum (AOS) shows peaks at every integer order. To generate a HI to differentiate between a healthy and faulty sample, the area under the RMS order spectrum is calculated for orders above 0.5. A faulty encoder is expected to have peaks at every order depending upon the severity level and therefore will have more area under the spectrum in comparison with healthy encoder as shown in Figure 7.

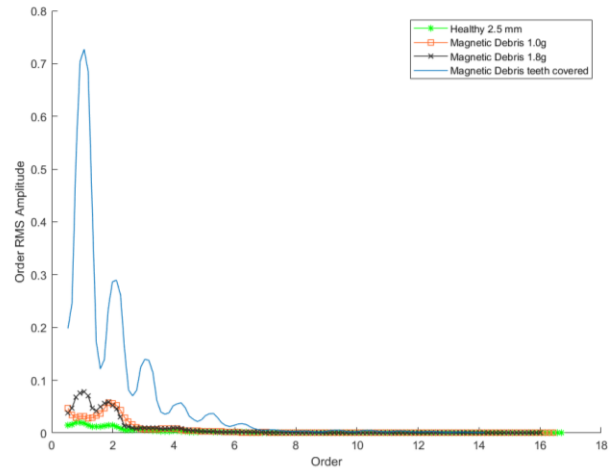


Figure 7. Average order spectrum of the wheel speed noise

### 3.2. Ground Truth

It is necessary to evaluate the severity levels of the fault injected samples. The severity levels of the samples are evaluated by using measure of median wheel noise over 110 kmph in rps and will act as a ground truth for regression modelling. Table 3 summarizes the various fault injected samples with fault severity levels.

Case ID	FaultMode	Ground Truth
97	Healthy 2.5 mm	0.01265
118	Healthy 1 mm	0.013
117	Healthy 1 mm	0.01345
121	Healthy 2 mm	0.01375
122	Healthy 2 mm	0.01418
213	Magnetic Debris 1.0g	0.02989
220	Magnetic Debris 0.6g	0.04533
218	Magnetic Debris 1.8g	0.04765
219	Magnetic Debris 0.6g	0.04795
217	Magnetic Debris 1.8g	0.04881
215	Magnetic Debris Teeth covered	0.03881

Table 3. Ground truth realization of faulty samples

### 4. RESULTS AND DISCUSSION

All the encoders are tested are tested using the UDDS (Urban Dynamometer Driving Schedule) speed cycle as shown in Figure 8. It is important to evaluate the performance of our HIs against change in speed and accelerations.

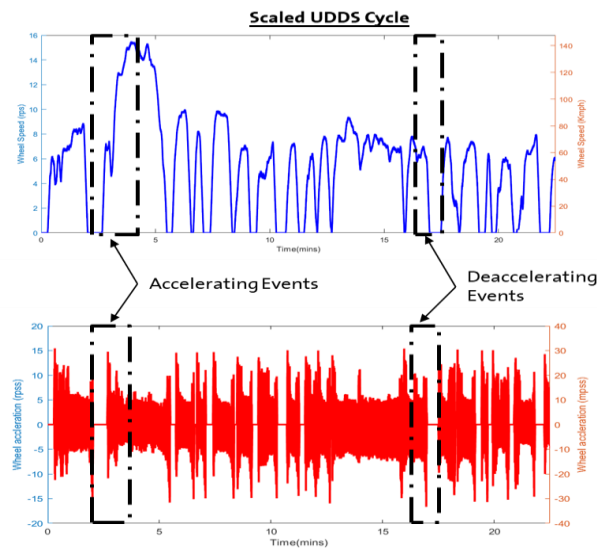


Figure 8. UDDS speed cycle (A), UDDS acceleration cycle (B)

Figure 9 shows the comparison of stitched wheel speeds and HI- LM bit 5,6 & 7 (Airgap) of various encoder samples with different amount of debris. The increase of debris build-up on the encoder reduced the magnetic strength from seven to lower values depending on the faulty encoder. The debris build up covering the edge of the wheel encoder shows unique signatures such that HI jitters and wheel speed is noisier in comparison to other encoders. Figure 9 also shows that the HI remains constant throughout the cycle and is independent to changes in wheel speed and accelerations.

#### 4.1.1. VDA

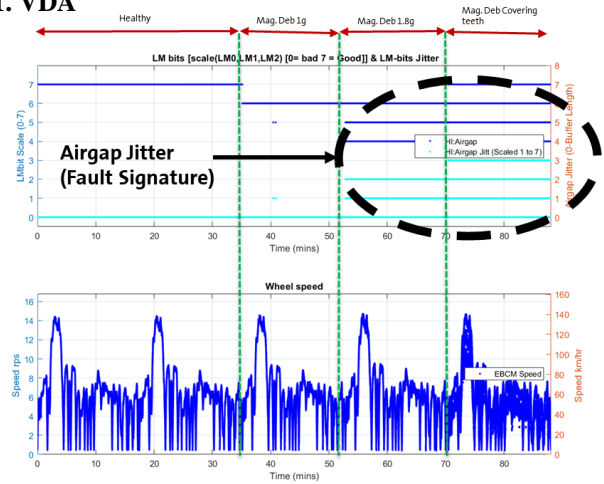


Figure 9. HI – LM bit 5,6, & 7 (Airgap) performance with different amount of contamination (A), Stitched wheel speeds with different amount of contamination (B)

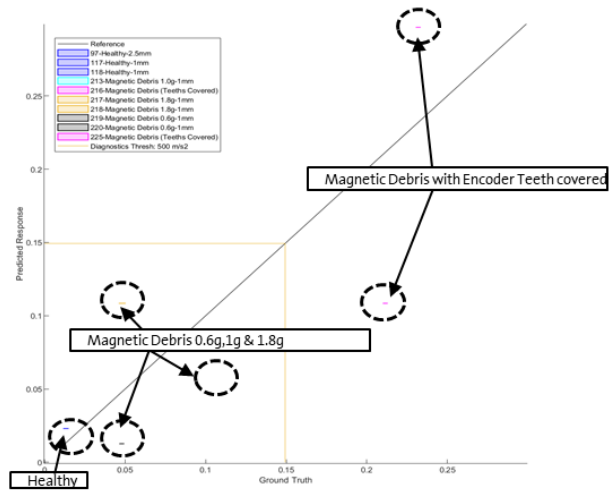


Figure 10. Regression performance of HI Airgap.

Figure 10 shows results of linear regression using HI Airgap as the predictor within speed range of 15kmph – 110kmph. This HI shows poor predictions for the contaminated encoder with RMSE of around 54.3e-3 rps.

Figure 11 compares wheel speed noise and acceleration levels between various encoders with different amount of contamination and healthy encoder. With the increase in the amount of contamination it is observed that wheel speed noise and acceleration levels increase as well. Magnetic debris covering the teeth shows unique signatures and stands out in comparison with other samples.



### 4.1.2. Envelope of Wheel Speed

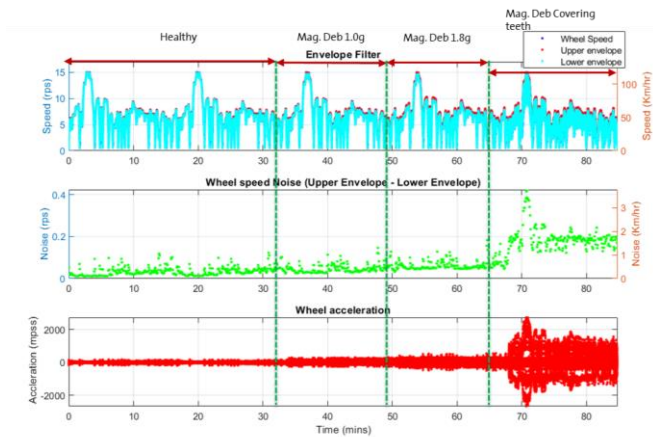


Figure 11. Stitched wheel speed with different amount of contamination (A), stitched wheel speed noise with different amount of contamination (B), stitched wheel acceleration with different amount of contamination (C)

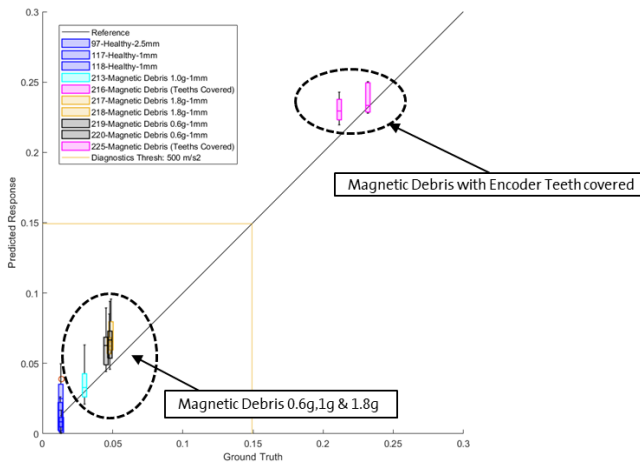


Figure 12. Regression performance of HI based on Wheel Noise.

Figure 12 shows regression results by using wheel noise-based HI. The prediction performance of this indicator is good in healthy and contaminated region but has high variance. Change in wheel speed and accelerations impact the performance of this concept. The performance is improved by enabling the HI between speed range 38– 95 Kmph with RMSE reducing to  $16.2e-3$  rps.

### 4.1.3. Order Analysis

Figure 7 illustrates the order amplitude of different contaminated samples. The order amplitude of contaminated encoders increases with the increase in debris amount. Moreover, debris covering the teeth shows high amplitude peaks in comparison to the other fault modes.

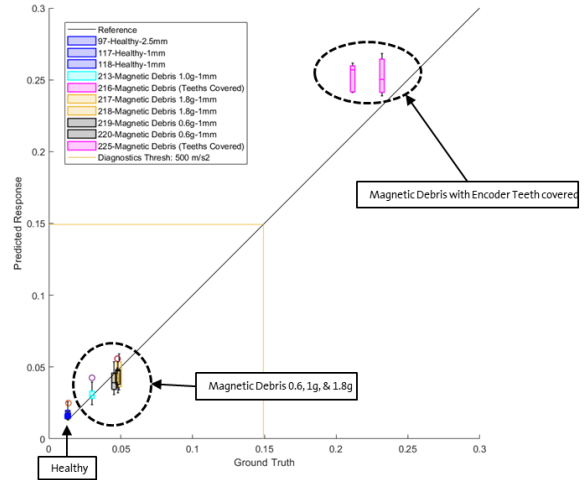


Figure 13. Regression performance of HI based on Order Spectrum.

Figure 13 shows the regression performance of HI based on order spectrum. This concept has low variance in comparison to the other two strategies with RMSE  $8.6e-3$  rps in speed range of 38-95 kmph. The prediction performance is impacted in the magnetic debris with teeth covered region. Moreover, this concept shows good separation between healthy and contaminated samples but not within the contaminated samples. The performance of this HI is impacted by the change in wheel speed and accelerations.

### 4.1.4. HI Fusion (VDA-Airgap + Wheel Noise-Envelope Filter + Wheel Noise-Order Analysis)

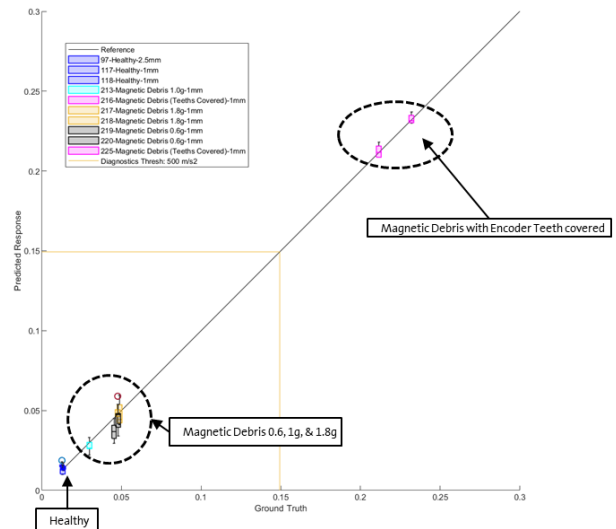


Figure 14. Regression performance of HI based on (VDA-Airgap + Wheel Noise-Enveloping Filter + Wheel Noise-Order Spectrum).

Each of these HI's performance limits the detection capability because of their individual limitations. Fusing VDAs binary and independent nature from change in wheel speed along with other speed dependent health predictors will improve their prediction performance.

Figure 14 illustrates the regression performance with the fused predictors VDA-Airgap, Wheel Noise-Envelope Filter and Wheel Noise-Order Spectrum. Fusion reduced the variance of the wheel speed-based HIs and improved the prediction performance in individual regions with RMSE  $4.5e-3$  rps as compared to the other HI's.

HIs discussed above quantifies defects in the WSS/Encoder interface in terms of noise. Any deterioration in the interface will be indicated by the HI depending on the severity levels. Therefore, in case of scenarios when particles fly off the surface of the encoder, the HIs will go back to healthy and fault will go away. Additionally, maturation of HIs can be tuned to take care of false positives and/ false negatives rates.

## 5. CONCLUSION

We tested various magnetic encoder samples with varying amount of debris to evaluate impact on the quality of the wheel speed signal. The results demonstrated that an increase in the amount of debris induces noise in the wheel speed signal and poses potential to jeopardize the performance of the vehicle.

HIs based on VDA-Airgap, Envelope Filter and Order analysis were developed to prognose the contamination level of the encoders and following conclusions were derived:

- HI based on VDA-Airgap demonstrated low potential to determine the debris level but is independent of change of wheel speed and accelerations.
- HI based on Wheel Noise-Envelope filter shows some potential to determine the debris level but considerable amount of overlap between fault levels. The performance also changes with change in wheel speed and accelerations.
- HI based on Wheel Noise-Order Analysis demonstrated good potential to determine the debris level and shows low variation in comparison to Wheel Noise-Envelope Filter. The performance of this HI is impacted with change in speed and acceleration.
- Fusing the information of VDA-Airgap with other HI's helped to reduce their variance and improved the overall performance in comparison to other individual HI's. This HI demonstrated higher potential than others to determine debris amount.

## ACKNOWLEDGEMENT

We thank Hossein Sadjadi-VHM Technical Specialist, Steven Weber- Brake and Control Systems Technical Specialist and Mohit Batra (formerly GM) Controls Development Engineer for their contribution in the project.

## NOMENCLATURE

<i>VDA</i>	Verband der Automobilindustrie
<i>WSS</i>	Wheel Speed Sensor
<i>EBCM</i>	Electronic Brake Control Module
<i>RMSE</i>	Root means square error
<i>ABS</i>	Antilock brake system
<i>TCS</i>	Traction control system
<i>ESC</i>	Electronic stability control
<i>HI</i>	Health Indicator
<i>FDI</i>	Fault detection and isolation
<i>HIL</i>	Hardware in loop
<i>rps</i>	revolution per second
<i>AOS</i>	Average order spectrum
<i>UDDS</i>	Urban Dynamometer Driving Schedule

## REFERENCES

- Savaresi, S. M., Tanelli, M., & Cantoni, C. (2006). Mixed slip-deceleration control in automotive braking systems. *Journal of Dynamic Systems, Measurement and Control, Transactions of the ASME*, 129(1), 20–31
- Oniz, Y., Kayacan, E., & Kaynak, O. (2009). A dynamic method to forecast the wheel slip for antilock braking system and its experimental evaluation. *IEEE Transactions on Systems, Man, and Cybernetics. Part B, Cybernetics*, vol. 39(2), pp. 551–560.
- Houhua Jing, Zhiyuan Liu, & Hong Chen. (2011). A switched control strategy for antilock braking system with on/off valves. *IEEE Transactions on Vehicular Technology*, 60(4), 1470–1484.
- Schwarz, R., Nelles, O., Scheerer, P., & Isermann, R. (1997). Increasing signal accuracy of automotive wheel-speed sensors by on-line learning. In *Proceedings of the Am. Control. Conference* (pp. 1131–1135).
- Hernandez, W. (August 2003). Improving the response of a wheel speed sensor by using frequency-domain adaptive filtering. *IEEE Sensors Journal*, 3(4), 404–413.
- Hernández, W. (April 2003). Improving the response of a wheel speed sensor using an adaptive line enhancer. *Measurement*, 33(3), 229–240.
- Bosch. (2014). *Encyclopedia of automotive. Engineering.* Wiley.
- Bosch. (2015). *basic technical documentation sensor DF30H.*
- Vachtsevanos, G., Lewis, F. L., Roemer, M., Hess, A., & Wu, B. (2006). *Intelligent fault diagnosis and prognosis for engineering system.* John Wiley & Sons, Inc.
- Pratama, P. S., Setiawan, Y. D., Kim, D. H. et al. (2014). Fault detection algorithm for automatic guided vehicle based on multiple positioning modules. In *Proceedings*

of the IEEE International Conference on Computing, Communications and Informatics (ICACCI 2014) (pp. 751–757).

Patton, R., Frank, P., & Clark, R. (2000). Issues of fault diagnosis dynamic systems. Springer.

Dadashnialehi, A., Bab-Hadiashar, A., Cao, Z., & Kapoor, A. (2013). Intelligent sensorless ABS for in-wheel electric vehicles. IEEE Transactions on Industrial Electronics, 61(4), 1957–1969.

#### BIOGRAPHIES

**Jasmeet S. Ladoiye** was born in India, 1992. He received the B.Tech in mechanical engineering from Lovely Professional University, 2014 and MaSc in mechanical engineering from University of Ottawa, 2018. He is currently working as a Controls Development Engineer with General Motors, Canada. His research interests include robotics & controls, AV's, signal processing and Internet of things.

**Douglas Spry** is an advanced chassis controls design engineer at General Motors working on the future of braking and brake controls. He is named on several pending patents

related to braking technologies. He holds a BS in Physics Research from Eastern Michigan University. Prior to working at General Motors Douglas focused on automated manufacturing as a robotics engineer with Jacobs Engineering Group and as the North American engineering lead for Lactec GmbH. His research interests include vehicle dynamics, AV service and reliability, and smart actuator design.

**Milad Jalali** received his B.S. and M.S. degree in Mechanical Engineering from Amirkabir University of Technology (Tehran Polytechnic) in 2008 and 2010; and the Ph.D. degree in Mechanical Engineering from University of Waterloo, Waterloo, ON in 2016. He is currently the development lead in Advanced Vehicle Prognostics team at General Motors (GM) Canadian Technical Center (CTC). His research interests include vehicle health management, vehicle dynamics, active vehicle safety control, and model predictive control.